Molecular Microbiology (2017) 103(5), 780–797

doi:10.1111/mmi.13589
First published online 10 January 2017

CtrA controls cell division and outer membrane composition of the pathogen *Brucella abortus*

Nayla Francis,[1] Katy Poncin,[1] Antonella Fioravanti,[2†] Victoria Vassen,[1] Kevin Willemart,[1] Thi Anh Phuong Ong,[1] Luca Rappez,[1‡] Jean-Jacques Letesson,[1] Emanuele G. Biondi[2,3] and Xavier De Bolle[1]*

[1]*Microorganisms Biology Research Unit (URBM), Narilis, University of Namur, Namur, Belgium.*
[2]*Unité de Glycobiologie Structurale et Fonctionnelle, UMR 8576 CNRS – Université de Lille, 50 Avenue Halley, Villeneuve d'Ascq, France.*
[3]*Laboratoire de Chimie Bactérienne, Institut de Microbiologie de la Méditerranée, Aix-Marseille Université, CNRS, UMR 7283, Marseille, France.*

Summary

Brucella abortus **is a pathogen infecting cattle, able to survive, traffic, and proliferate inside host cells. It belongs to the *Alphaproteobacteria*, a phylogenetic group comprising bacteria with free living, symbiotic, and pathogenic lifestyles. An essential regulator of cell cycle progression named CtrA was described in the model bacterium *Caulobacter crescentus*. This regulator is conserved in many alphaproteobacteria, but the evolution of its regulon remains elusive. Here we identified promoters that are CtrA targets using ChIP-seq and we found that CtrA binds to promoters of genes involved in cell cycle progression, in addition to numerous genes encoding outer membrane components involved in export of membrane proteins and synthesis of lipopolysaccharide. Analysis of a conditional *B. abortus ctrA* loss of function mutant confirmed that CtrA controls cell division. Impairment of cell division generates elongated and branched morphologies, that are also detectable inside HeLa cells. Surprisingly, abnormal bacteria are able to traffic to the endoplasmic reticulum, the usual replication niche of *B. abortus* in host cells. We also found that CtrA depletion affected outer membrane composition, in particular the abundance and spatial distribution of Omp25. Control of the *B. abortus* envelope composition by CtrA indicates the plasticity of the CtrA regulon along evolution.**

Accepted 23 November, 2016. *For correspondence. E-mail xavier.debolle@unamur.be; Tel. (+32) 81 72 44 38; Fax (+32) 81 72 42 97. Present addresses: †Structural Biology Research Center, VIB, Vrije Universiteit Brussels, Brussels, Belgium ‡European Molecular Biology Laboratory (EMBL), Structural and Computational Biology Department, Heidelberg, Germany

Introduction

Brucella abortus is a facultative intracellular pathogen (Moreno and Moriyon, 2006) preferentially infecting cattle, although humans can be accidental hosts. Infection by *B. abortus* causes a disease called brucellosis, a worldwide zoonosis. *B. abortus* can infect both epithelial cells (such as HeLa and Vero cells) (Detilleux *et al.*, 1990) and professional phagocytes (macrophages and dendritic cells) (Archambaud *et al.*, 2010). Once inside host cells, *B. abortus* resides in a membrane-bound compartment called BCV for *Brucella* containing vacuole. *B. abortus* intracellular trafficking is biphasic; in a first a non-proliferative phase the BCV interacts with early and then late endosomes (Pizarro-Cerda *et al.*, 1998a; Chaves-Olarte *et al.*, 2002; Starr *et al.*, 2008), as shown by the acquisition of Lamp1, a marker of late endosomes and lysosomes. Then, in most cell types (Salcedo *et al.*, 2013), the second phase is characterized by bacterial proliferation in a compartment harboring endoplasmic reticulum (ER) markers (Pizarro-Cerda *et al.*, 1998a; Celli *et al.*, 2003; 2005). After this proliferation step, BCVs can acquire autophagic markers and bacteria spread to neighboring cells (Starr *et al.*, 2012).

Recently, new evidence showed that cell cycle and virulence of *B. abortus* are coordinated (De Bolle *et al.*, 2015; Deghelt *et al.*, 2014). *B. abortus* cell cycle starts with cell division, that generates two unequal daughter cells (Van der Henst *et al.*, 2013). Each daughter cell has a period in which chromosome replication is not initiated, they are proposed to be at the so-called G1 stage. When the chromosomal replication has started, the bacteria are at the S (DNA synthesis) phase. The stage between the end of chromosomal replication and cell division is G2. We recently developed tools to identify *B. abortus* at the G1 stage, at the single cell level (Deghelt *et al.*, 2014). Bacteria in the G1 stage of their

cell cycle are more infectious than their counterparts in S or G2 phases (Deghelt *et al*., 2014). Furthermore, during the early non-proliferative phase of the infection, bacteria remained in G1 phase for up to 6 h and were arrested for their growth (Deghelt *et al*., 2014). *B. abortus* is thus able to block its cell cycle while trafficking through the endocytic pathway. Around 8 h post-infection (PI) in HeLa cells, bacteria resumed chromosome replication and growth while still residing in Lamp1+ compartments. However, the newly generated daughter cells were delivered into Lamp1- BCVs (Deghelt *et al*., 2014).

Brucella abortus is a member of the *Alphaproteobacteria* class, and many key regulators controlling the cell cycle progression of the model organism *Caulobacter crescentus* are conserved in *B. abortus* (Hallez *et al*., 2004; Brilli *et al*., 2010). In particular the response regulator and transcription factor CtrA is exclusively present in *Alphaproteobacteria* and well conserved among them (Brilli *et al*., 2010). In *C. crescentus* this transcription factor controls the expression of genes involved in polar morphogenesis, division, DNA methylation and chemotaxis (Quon *et al*., 1998; Reisenauer *et al*., 1999; Laub *et al*., 2002). CtrA also binds the replication origin of *C. crescentus* chromosome, thereby preventing the initiation of its replication (Quon *et al*., 1998). CtrA regulates similar processes in *Sinorhizobium meliloti*, a symbiont of legume plants (Pini *et al*., 2015). In these two microorganisms, CtrA amount oscillates during cell cycle thanks to regulations occurring at multiple levels (Domian *et al*., 1997; Holtzendorff *et al*., 2004; Pini *et al*., 2015). In *B. abortus*, DNase I footprinting assays suggested that CtrA is also involved in cell cycle regulation as it is able to bind the promoter of *ccrM* coding for an essential DNA methyltransferase (Robertson *et al*., 2000), and promoters of *ftsE* and *minC* genes, that are involved in division (Bellefontaine *et al*., 2002). CtrA also binds its own promoter (Bellefontaine *et al*., 2002). In *C. crescentus* CtrA recognizes two consensus sequences, the "TTAA(N_7)TTAAC" 9-mer box (Quon *et al*., 1998) and the "TTAACCAT" 8-mer box (Laub *et al*., 2002), which are also found in predicted CtrA target promoters in *B. abortus* (Bellefontaine *et al*., 2002; Hallez *et al*., 2004).

At the post-translational level, phosphorylation and proteolysis of CtrA are controlled by a complex network (Curtis and Brun, 2010) that is predicted to be conserved in many *Alphaproteobacteria* (Brilli *et al*., 2010). The phosphorylation cascade controlling CtrA activity in *B. abortus* is conserved and functional (Willett *et al*., 2015). Alteration of CtrA control generates defects in intracellular survival and a shift in the abundance in *ccrM* transcripts (Willett *et al*., 2015). However, the regulon of CtrA in *B. abortus* was poorly explored until now.

Here, we investigated the regulon of *B. abortus* CtrA by performing a chromatin immunoprecipitation followed by deep sequencing (ChIP-seq) analysis. A detailed analysis of CtrA binding sites on *B. abortus* genome not only revealed that CtrA binds to the promoters of genes involved in cell cycle control and progression, but it also binds to the promoters of genes involved in biogenesis of the outer membrane. We show that CtrA is dispensable for elongation but is essential for division, CtrA absence generating large branched morphologies both in culture and inside host cells. Moreover, CtrA is involved in the control of outer membrane composition. Finally, we show that the activity of two CtrA-bound promoters change according to bacterial cell size, suggesting that CtrA is indeed a cell cycle regulator.

Results

Investigating the CtrA regulon by ChIP-seq

Since CtrA was recently proposed to control *B. abortus* cell cycle (Bellefontaine *et al*., 2002; Willett *et al*., 2015), a ChIP-seq analysis was performed to map CtrA binding sites on *B. abortus* 544 genome, when this bacterium is grown in rich medium until the mid-exponential phase. The ChIP-seq data and the annotated Genbank files are available as Supplemental material (Chr1.gb, ChIP-seq_CtrA_chr1.txt, Chr2.gb and ChIP-seq_CtrA_chr2.txt files). From this analysis, 109 CtrA binding regions were selected (Supporting Information Table S1). CtrA binding sites are scattered on the two chromosomes (Supporting Information Fig. S1). Of these regions, 71% had a predicted 9-mer or 8-mer consensus binding site with 0, 1, or 2 mismatches, and 97% mapped to intergenic regions. Among the CtrA-bound sequences with no predicted 9-mer or 8-mer box, 57% had at least one "TTAA(C)" half site. CtrA binding pattern to DNA showed a single peak coinciding with a predicted binding site upstream of *cpdR* (BAB2_0042) and *ccrM* (BAB1_0516) (Fig. 1). CtrA binding upstream of its own promoter showed two peaks of equal size overlapping multiple consensus sequences (Fig 1). These peaks corresponded to the regions protected from DNase I digestion by purified phosphorylated CtrA in an *in vitro* assay (Bellefontaine *et al*., 2002). It should be noted that this intergenic region bound by CtrA could also serve to regulate the expression of another gene (BAB1_1615), which has an opposite orientation to *ctrA* (BAB1_1614). Similarly, CtrA binding between BAB2_1162 and *repA* (BAB2_1163, a gene putatively involved in the segregation of chromosome II replication origins) had a double peaks pattern, but the peaks were of unequal size, and the apparently stronger binding site contains a half site

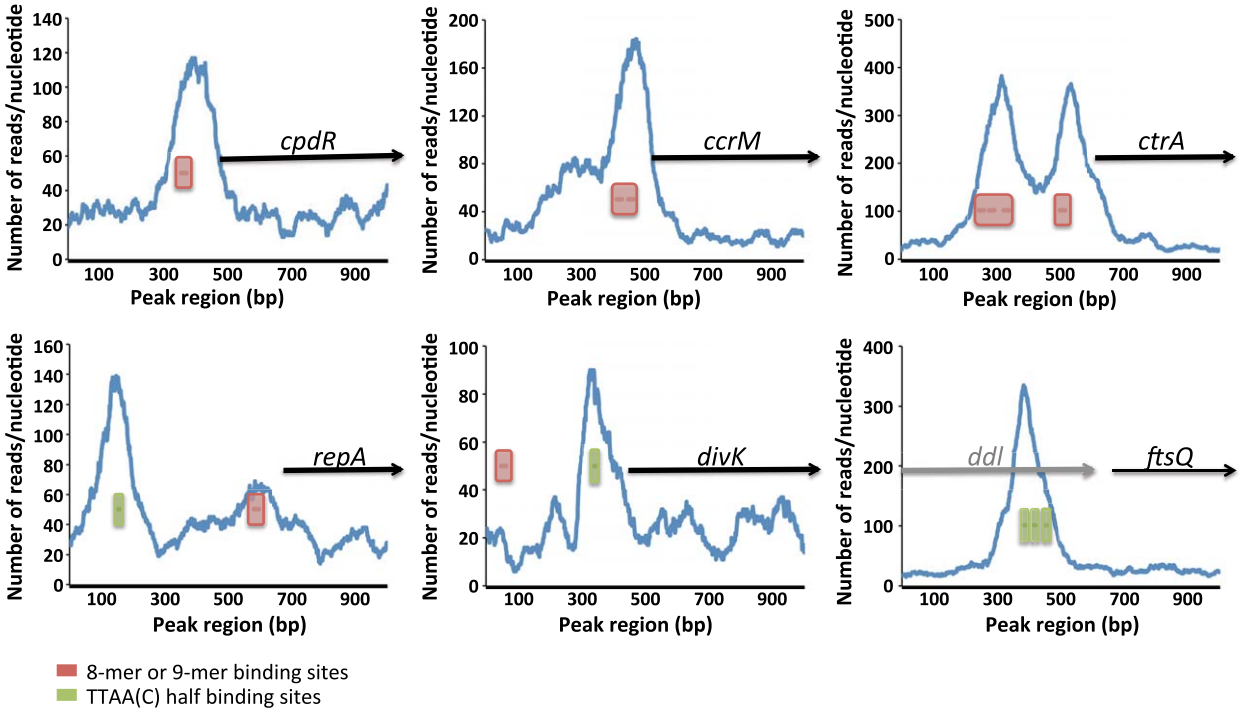

Fig. 1. *In vivo* CtrA binding sites detected by ChIP-seq. The number of reads per nucleotide is plotted for six promoter regions enriched by CtrA pull-down. Red bars surrounded by red rectangles represent predicted 8-mer and 9-mer binding sites. Green bars surrounded by green rectangles represent TTAA(C) half binding sites. Arrows under gene names represents the start of the coding sequences.

TTAAC (Fig. 1). Some other CtrA binding patterns to DNA were less expected. For instance, CtrA bound a region upstream of *divK* (BAB2_0628, coding for a regulator of cell cycle (Hallez *et al.*, 2007b; Mignolet *et al.*, 2010)) at the level of a TTAAC half site despite the presence of a 9-mer box around 300 base pairs upstream the actual binding site (Fig. 1). CtrA also bound a region inside the *ddl* open reading frame (BAB1_1447), which is in operon with *ftsQ*, *ftsA*, and *ftsZ*. Ddl is a D-Ala-D-Ala ligase while FtsQ, FtsA, and FtsZ are cell division proteins. Interestingly, this binding site overlaps three TTAAC half sites. A similar binding profile was observed in *C. crescentus*, where CtrA also bound a sequence within the *ddl* gene upstream of the *ftsQA* operon (Laub *et al.*, 2002).

The direct binding of CtrA to promoters identified in ChIP-seq was confirmed by an electrophoretic mobility shift assay (EMSA), using *minC*, *dnaA*, *ftsQ*, *bamA*, *omp25*, and *tolQ* promoters as probes (Supporting Information Fig. S2), suggesting that –at least in the case of these target genes– CtrA alone is able to directly bind these promoters.

The genome-wide analysis of the functional classes of CtrA-targeted genes revealed an enrichment of genes involved in cell cycle (cell division, replication, DNA methylation, and cell cycle control) as expected, but also numerous genes involved in envelope biogenesis/homeostasis. Indeed, genes predicted to be involved in envelope composition and cell cycle are significantly enriched among CtrA targets, as they constitute 33.3% and 11.5% of CtrA regulon respectively compared with 3.3% and 2.6% of the whole genome of *B. abortus* ($p < 0.001$ in a χ^2 analysis).

CtrA is predicted to directly control many genes involved in cell division (Supporting Information Table S1). These include the *minCDE* operon coding for the Min system (Meinhardt and de Boer, 2001), whose function is to control the mid-cell placement of the Z ring. This role in Z ring placement is in agreement with the MinD oscillation reported in *B. abortus* (Hallez *et al.*, 2007a). The promoters of the genes coding for proteins involved in Z ring formation and subsequent constriction (*ftsQAZ*, *ftsB*, *ftsEX*) are also directly bound by CtrA. The genes (*pal* and *tolQRAB*) coding for proteins involved in the invagination of the outer membrane during cell division (Gerding *et al.*, 2007) are also direct targets of CtrA, suggesting that CtrA potentially controls the whole cell division process. CtrA is also binding the promoters of genes or operons involved in dNTP synthesis (*nrdHIEF*), the initiation of chromosome I replication (*dnaA*), the partition of chromosome II origins (*repAB*) (Deghelt *et al.*, 2014), and the segregation of chromosomes at the termination of replication (*ftsK*) (Stouf *et al.*, 2013).

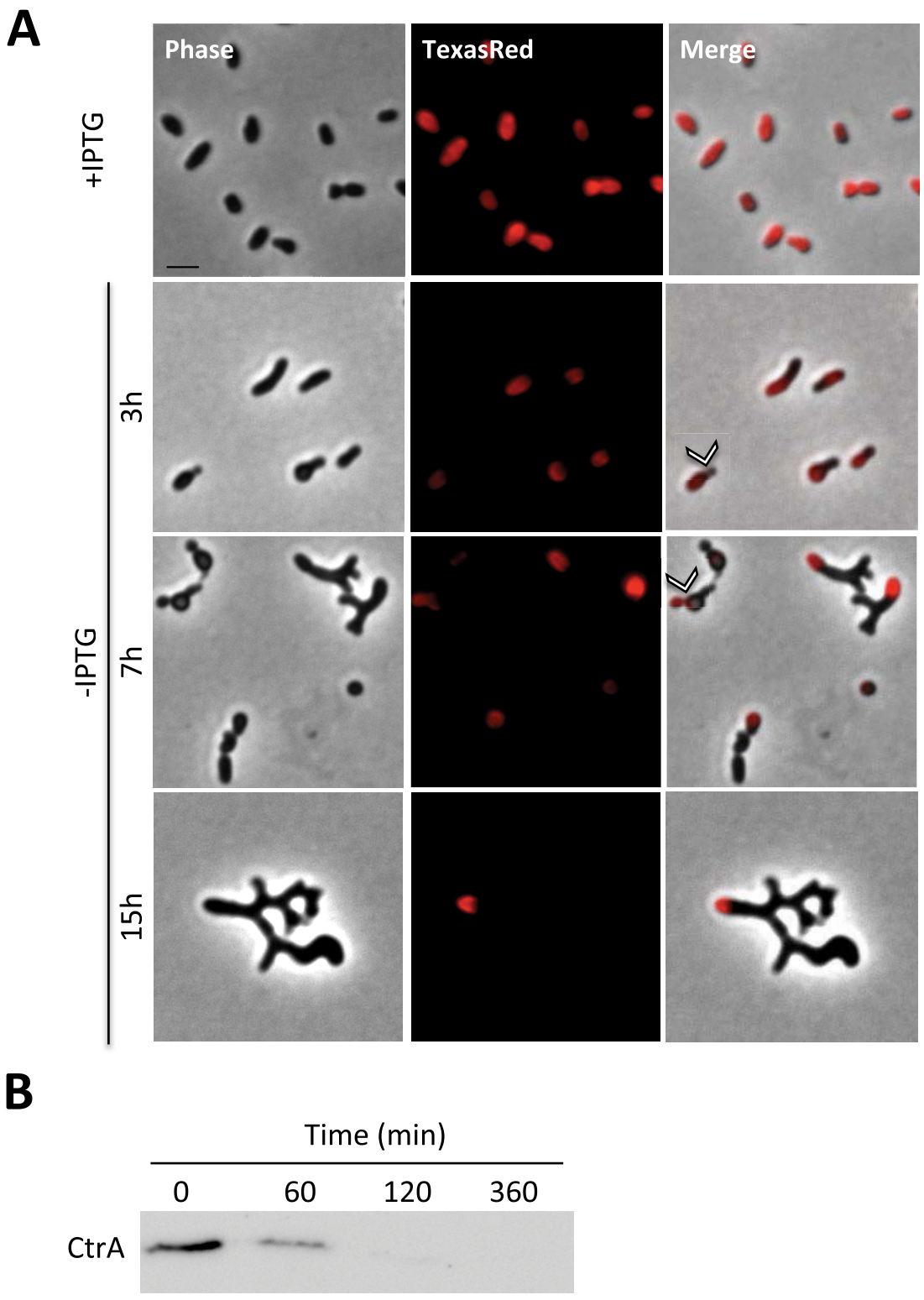

Fig. 2. CtrA depletion generates cell division defects strain in *B. abortus*.
A. Phase contrast ("Phase") and fluorescence ("TexasRed") microscopy images of a CtrA depletion strain labeled with TRSE and grown with IPTG ("+IPTG") show that bacteria have a normal morphology. Upon IPTG removal ("−IPTG"), bacteria elongate (3 h), form chains and branch (7 and 15 h). TRSE allows covalent binding of amine groups present at the bacterial surface to Texas Red. Growth occurring after TRSE labeling results in the incorporation of unlabeled envelope material. The scale bar corresponds to 2 μm.
B. CtrA detection by Western blot shows a quick decrease in CtrA amount and apparent clearance 120 min post-IPTG removal.

CtrA is binding many *B. abortus* promoters involved in envelope composition (Supporting Information Table S1). Indeed, it is targeting genes involved in LPS biosynthesis (*lpxD-fabZ-lpxAB* and *lpxE*), LPS export to the OM (*lptAB* and *lptFGD*), OM proteins composition (*omp2b*, *omp25*, *ropB*, *omp19*, BAB1_0045, BAB1_0075, BAB1_1701, and BAB2_0314) and the incorporation of proteins into the OM (*bamA*). Moreover, CtrA binds to the promoter of six genes coding for L, D-transpeptidases homologs (BAB1_0047, BAB1_0138, BAB1_0589, BAB1_0978, BAB1_1159, BAB1_1867), enzymes that link m-Dap residues within the peptidoglycan mesh (Magnet *et al.*, 2008). The function of these L, D-transpeptidases is unexplored in *B. abortus*, but one of these L, D-transpeptidases (homologous to BAB1_0589) was found to be localized at the growth pole in *Agrobacterium tumefaciens* (Grangeon *et al.*, 2015). PopZ is also localized at the growth pole in *B. abortus* (Deghelt *et al.*, 2014) and *A. tumefaciens* (Grangeon *et al.*, 2015), and its gene is also a direct target of CtrA in *B. abortus*. These observations suggest that polar differentiation could be controlled by CtrA in *B. abortus*.

One striking feature of the CtrA regulon in *B. abortus* is the high proportion of genes encoding proteins involved in the control of CtrA. As depicted in Supporting Information Fig. S3, the *divJ*, *divK*, *divL*, *chpT*, *cpdR*, *rcdA*, *sciP*, and *ccrM* genes are proposed to control CtrA, but our data also suggest that these genes are direct targets of CtrA, highlighting the potential circular topology of this regulation network, consistent with cell cycle control. CtrA was reported to control *ccrM* transcripts levels in *B. abortus* (Willett *et al.*, 2015), which is consistent with its binding to the *ccrM* promoter *in vitro* (Bellefontaine *et al.*, 2002) and *in vivo* (Supporting Information Table S1). It is noteworthy that enrichment of reads at the *dnaA* promoter is weak, suggesting either CtrA binding is infrequent or it happens only in a small fraction of the bacterial population.

It is also worth mentioning that only few genes proposed to encode virulence factors are directly bound by CtrA. These include a manganese transporter gene *mntH* (Anderson *et al.*, 2009) and a periplasmic superoxide dismutase gene *sodC* (Gee *et al.*, 2005). CtrA proposed direct targets also comprise the main transcriptional regulator of flagellar genes (*ftcR*) (Leonard *et al.*, 2007) and several putative DNA repair genes (*uvrC*, *addBA*, *mutM*, and *tagA*).

We decided to further investigate the role of CtrA in regulating cell division and envelope composition by constructing a CtrA depletion strain and analysing its phenotype in culture and in the context of a cellular infection.

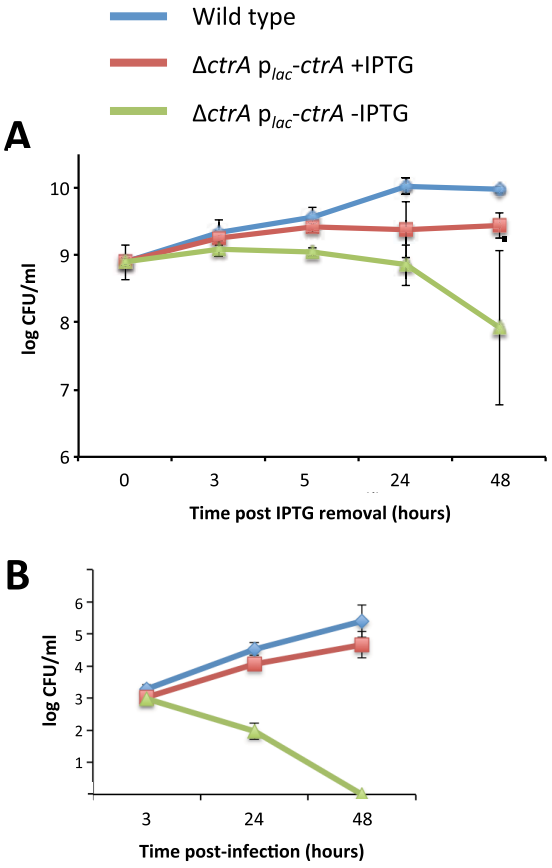

Fig. 3. Viability of the CtrA depletion strain in rich medium and infection.
A. CFU count of wild type and CtrA depletion (Δ*ctrA* p$_{lac}$-*ctrA*) strains cultivated with or without IPTG (+IPTG or −IPTG, respectively) in rich medium. Error bars correspond to standard deviations ($n = 3$).
B. CFU count of wild type and CtrA depletion (Δ*ctrA* p$_{lac}$-*ctrA*) strains incubated with or without IPTG (+IPTG or −IPTG, respectively) during a HeLa cell infection over a 48 h period of time. Standard deviations are shown ($n = 3$).

CtrA is crucial for B. abortus *cell division*

In *C. crescentus*, CtrA is the master regulator controlling many important genes required for cell cycle progression. Here we investigated the *B. abortus* CtrA function *in vivo* by generating a *ctrA* depletion strain, as this gene was suggested to be essential (Bellefontaine *et al.*, 2002). First, a wild type (WT) copy of *ctrA* was cloned on a replicative plasmid as a fusion with an IPTG-inducible promoter; then the chromosomal *ctrA* deletion was obtained by allelic replacement in the presence of IPTG. When the growth medium was supplemented with IPTG, the Δ*ctrA* p$_{lac}$-*ctrA* strain harbored a WT morphology (Fig. 2A). Upon IPTG removal, CtrA was cleared within 2 h from the cells (Fig. 2B). Abnormal morphologies appeared from 3 h post IPTG removal and consisted of elongated cells and cells with

mislocalized constrictions (Fig. 2A). At 3 h post-IPTG removal, a fraction of CtrA-depleted bacteria (10.9%) were longer than 2.75 μm while only 1.6% of WT bacteria and 1.3% of the depletion strain grown with IPTG exceeded this size ($p < 0.05$). A highly significant proportion ($p < 0.01$) of CtrA-depleted bacteria (6.3%) had a mislocalized constriction, i.e. detectable septa located very close to one pole (Fig. 2A; white arrow heads), compared with the WT strain (0.88%) and to the CtrA depletion strain grown with IPTG (1.33%) (Fig. 2A). Seven hours after IPTG was removed from the culture, we observed bacteria that grew to form multiple branches while others generated small chains, interpreted as filamentation with aborted divisions segmenting the bacteria (Fig. 2A). If the incubation in a CtrA-depleted state is prolonged (15 h), bacteria kept on branching. These results suggest that in the absence of CtrA, bacterial elongation is maintained but division is highly perturbed, since it is either abolished (there are almost no visible constriction sites in branching bacteria) or division is initiated at various positions but it is often not completed since bacteria form chains.

We next characterized the viability of the CtrA depletion strain. The viability of the CtrA depletion strain in rich culture medium was assessed by counting the number of colony forming units (CFU) (Fig. 3A). In these assays, colonies were grown on plates in the presence of IPTG, since this strain does not grow on plates without IPTG, consistent with the essentiality of the *ctrA* gene. When the CtrA depletion strain was cultivated in the presence of IPTG in liquid medium, a stable number of CFU was reached earlier than the WT control, and the plateau was lower (Fig. 3A). In the absence of IPTG, the number of CFU did not increase, and remained constant for 24 h before decreasing (Fig. 3A). The high variability of CFU numbers after 48 h of depletion (Fig. 3A) could be due to a high variability in the capacity of branched bacteria to divide and release viable bacteria. These data suggest that CtrA is essential for *B. abortus* growth and long-term survival in rich medium.

To test the reversibility of the CtrA depletion on cell division, the CtrA depletion strain was grown overnight without IPTG, labeled with Texas Red Succinimidyl Ester (TRSE) and inoculated in fresh medium supplemented with IPTG. The newly incorporated envelope appears unlabeled with TRSE after growth and thus new division sites appear as unlabeled rings (Brown *et al.*, 2012). After 3 h of repletion, we observed a reaccumulation of CtrA (Supporting Information Fig. S4A) and several unlabeled constriction sites were visible on the large bacteria (Supporting Information Fig. S4B). Six hours after IPTG was added to the medium, several division events were completed as shown by the release of unlabeled or partially labeled bacteria (Supporting Information Fig. S4B). Those bacteria were of different size and shapes, demonstrating that the septa were formed at ectopic sites. These results further confirm that CtrA is essential for division in *B. abortus*, and that CtrA depletion effect is reversible for the generation of cell division events, but not for their correct positioning in the cell. It also indicates that large branching bacteria generated in the absence of IPTG are not dead, at least after an overnight depletion of CtrA.

In the ChIP-seq study reported above, only one condition was tested, and it is likely that CtrA could be able to bind other targets in different conditions. Moreover is it also likely that CtrA could be a crucial regulator in a fraction of its targets, but only an accessory regulator for other promoters. The availability of a depletion strain for CtrA allowed us to test some CtrA targets promoters for their dependence on CtrA. Using reverse transcription followed by quantitative PCR (RT-qPCR), we found that the abundance of *ccrM* transcript is strongly dependent on CtrA since after a CtrA depletion condition (without IPTG) of 6 h, there is a significant ($p < 0.01$) 17.1 (± 0.8) fold decrease of *ccrM* mRNA abundance compared with the control condition (with IPTG). RT-qPCR analysis of other predicted CtrA targets (*omp25* and *ftsEX*) revealed statistically relevant changes in mRNA abundance, but of very low amplitude (typically <40%), highlighting the complexity of the regulation network involving CtrA.

The activity of CtrA target promoters varies in function of bacterial cell size

Since CtrA is a cell cycle regulator in *C. crescentus* (Quon *et al.*, 1998; Reisenauer *et al.*, 1999; Laub *et al.*, 2002) and *S. meliloti* (Pini *et al.*, 2015), we wondered if CtrA is also able to regulate its targets according to cell cycle. Because *B. abortus* is not synchronizable as of yet, we monitored the activity of CtrA target promoters at the single cell level, and we then sorted bacteria according to their size to reconstruct their cell cycle. A reporter system was designed to monitor the activity of *ccrM* (p_{ccrM}), *repAB* (p_{repAB}), *ctrA* (p_{ctrA}), and *pleC* (p_{pleC}) promoters by fusing each of them to a gene coding for an unstable GFP (GFP-ASV) (Andersen *et al.*, 1998) on a medium-copy replicative vector (Terwagne *et al.*, 2013). The *ccrM* and *ctrA* transcription follows a tightly regulated profile throughout *C. crescentus* cell cycle while PleC protein amount remains stable (Zweiger *et al.*, 1994; Quon *et al.*, 1996; Wheeler and Shapiro, 1999). The *repAB*, *ctrA*, and *ccrM* promoters are bound by CtrA in the ChIP-seq (Supporting

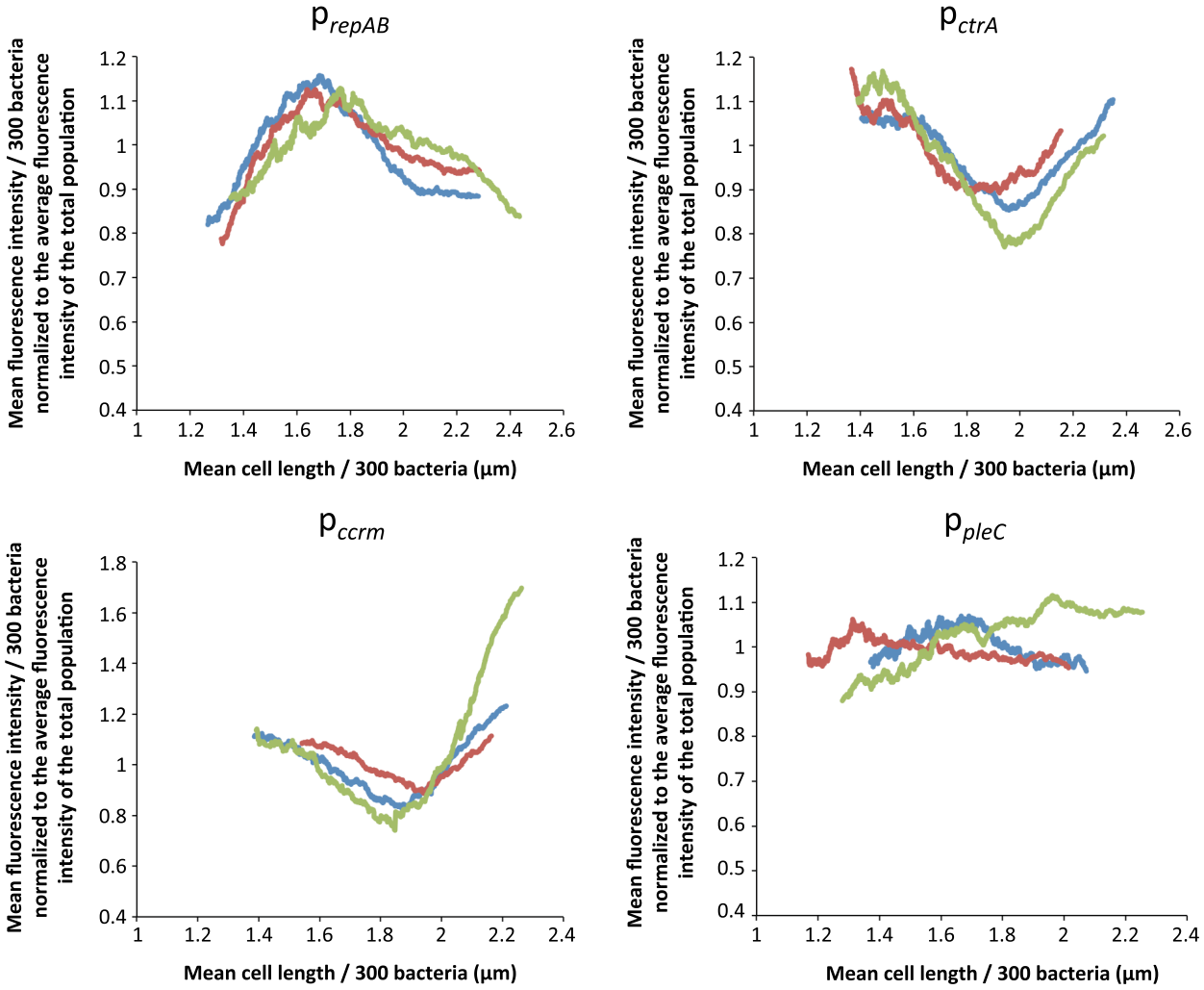

Fig. 4. Activity profile of *repAB, ctrA*, *ccrM* and *pleC* promoters according to cell length.
Phase and fluorescence microscopy images of *B. abortus* reporter strains were analyzed with the MicrobeTracker program. Bacteria were ordered according to their cell length and the mean cell length and mean fluorescence intensity was calculated for a sliding window (from smallest to largest bacteria) of 300 bacteria. The mean fluorescence intensities were normalized to the average fluorescence intensity of the whole population of a given experiment, allowing the representation of results from three independent experiments on the same plot. Each experiment is shown with a different color. The number of bacteria analyzed for p_{repAB} are 1632, 1402, and 2377; for p_{ctrA} 1456, 1487, and 1467; for p_{ccrM} 1446, 753, and 1678; for p_{pleC} 1888, 1297, and 1953.

Information Table S1), while the *pleC* promoter is not, at least in the conditions tested here.

Currently, unlike *C. crescentus* cell cycle, the *B. abortus* cell cycle is not synchronizable. To test if *ctrA*, *ccrM*, *repAB*, and *pleC* promoters are controlled along cell cycle, fluorescence intensity of the *B. abortus* reporter strains was measured in three independent experiments and mean fluorescence intensity was plotted against bacterial cell size (Fig. 4). The p_{ctrA} and p_{repAB} activities changed according to cell length, and they display opposite profiles as maximal fluorescence intensity was measured in intermediate bacteria for p_{repAB} and in small and large bacteria for p_{ctrA} reporters. These data suggest that p_{ctrA} activity is maximal in large dividing bacteria, and this activity decreases after division (Fig. 4). The maximal activity of p_{ctrA} in large bacteria is consistent with cell division defect in the CtrA depletion strain (Fig. 2). On the contrary, p_{repAB} seems to be turned on early in the cell cycle, leading to an accumulation of GFP-ASV in intermediate bacteria (Fig. 4). These data correlate with the initiation of replication of chromosome II at about half of the cell cycle of *B. abortus* (Deghelt *et al.*, 2014). The p_{ccrM} activity profile is similar to p_{ctrA} (Fig. 4); differences between bacterial length classes are however not significant, probably due to the high variability of fluorescence intensity between experiments, while variations of p_{repAB} and p_{ctrA} activities according to cell length were significant (Supporting

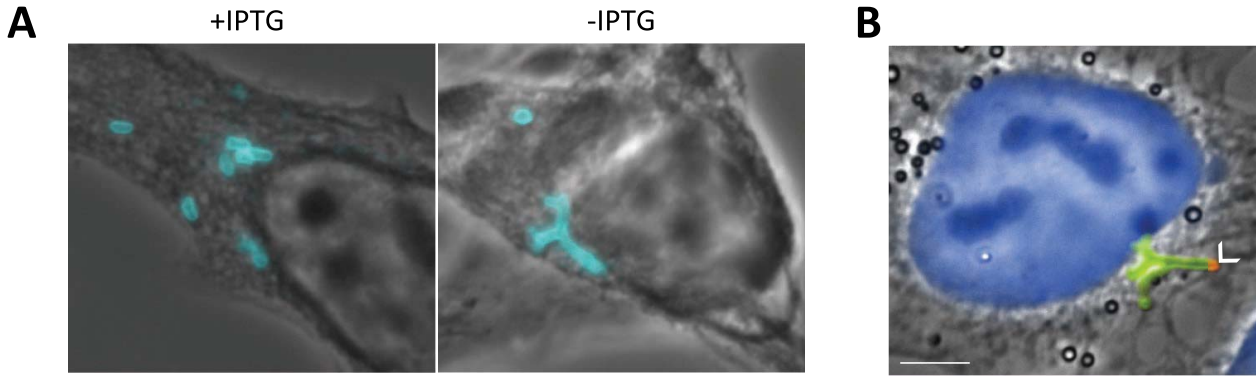

Fig. 5. Morphology of the CtrA depletion strain during infection.
A. Immunofluorescence microscopy of HeLa cells infected for 15 h with the depletion strain in presence or in absence of IPTG. Phase contrast images were merged with anti-*Brucella* staining (cyan) to detect intracellular bacteria. The scale bars correspond to 5 μm. The absence of IPTG, bacteria with normal and abnormal morphologies can be found in variable proportions from one infection to the other.
B. Representative image of an abnormal morphology generated by the CtrA depletion strain 15 h post-infection in HeLa cells, with bacteria labeled with TRSE before infection. The TRSE-labeled part corresponds to the old pole of the initial bacterium that invaded the host cell (white arrow head). DAPI (staining the nucleus in blue), anti-*Brucella* (green) and Texas Red are merged.

Information Fig. S5). The p_{pleC} did not show any significant variation in its activity according to bacterial cell size (Fig. 4 and Supporting Information Fig. S5). Taken together, these data suggest that two promoters bound by CtrA *in vivo* are differentially regulated during *B. abortus* cell cycle, supporting the role of CtrA as a cell cycle regulator.

The *ccrM* and *repAB* promoters contain two and one proposed CtrA binding sites respectively (Supporting Information Fig. S6). Using the p_{ccrM}-gfp_{asv} and p_{repAB}-gfp_{asv} fusions cited above, we created mutants in the CtrA binding boxes (Supporting Information Fig. S6) and we were able to show that mutagenesis of CtrA binding box 2 for p_{ccrM} and mutagenesis of the CtrA binding box in p_{repAB} abolished activity of these promoters, strongly suggesting that CtrA is crucial to activate them. Of course, we cannot exclude that these mutations also impair the binding of other crucial factors required for the activity of *repAB* and *ccrM* promoters. The mutation of CtrA binding box 1 in p_{ccrM} did not yield a significant effect, suggesting that its role is either subtle or restricted to a condition that was not present in our experiments.

CtrA is required for B. abortus *division and survival in HeLa cells*

To assess the role of CtrA during infection, the depletion strain was used to infect HeLa cells. Bacteria were incubated with HeLa cells for 1 h with IPTG. Cells were then washed and gentamicin was added to kill extracellular bacteria. The CtrA depletion strain was able to infect HeLa cells and to replicate intracellularly almost to the same extent as the WT when IPTG was kept in the medium (Fig. 3B). When IPTG was removed after the initial hour of internalization, a similar number of CFU was recovered 3 h PI, and then the CFU counts dropped dramatically and went below the detection limit at 48 h PI. We verified that the presence of Triton X-100, used for the extraction of bacteria from host cells, did not decrease the CFU counts for the CtrA depletion strain in the absence of IPTG (Supporting Information Fig. S7). Altogether, these data suggest that CtrA is crucial for *B. abortus* viability during HeLa cells infection.

Similarly to the rich medium condition, we analyzed the morphology of the CtrA depletion strain during infection. As expected, this strain had WT morphology when IPTG was kept in the medium (Fig. 5A). When the infection was performed in the absence of IPTG, bacteria with aberrant morphologies appeared from 10h PI, but their proportion was variable from one infection to the other. The intracellular branched morphologies are similar to those observed after a long depletion in culture (Fig. 2). If bacteria are labeled with TRSE prior to infection, they also display a Texas Red fluorescence at the base of the branched morphology (Fig. 5B; white arrow head). The emergence of abnormal morphologies late in the trafficking is consistent with the previously reported biphasic trafficking of *B. abortus* in HeLa cells (Deghelt *et al.*, 2014). Indeed, *B. abortus* intracellular growth is detected between 6 and 8 h PI in HeLa cells, suggesting a growth arrest of at least 6 h (Deghelt *et al.*, 2014). The CtrA depletion generates elongated morphologies at 10 h PI, suggesting that growth was also arrested for several hours before, otherwise these abnormal morphologies would have appeared around 3 h PI. This suggests that CtrA is not crucial to control the timing of the intracellular growth recovery.

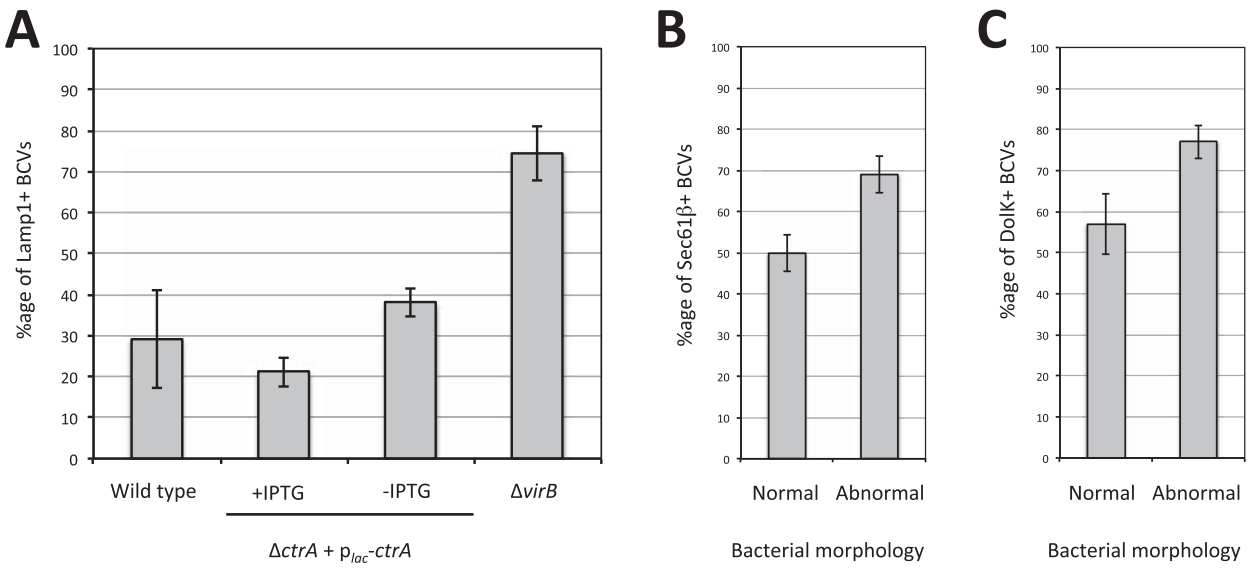

Fig. 6. Intracellular trafficking of the CtrA depletion strain.
A. Three *B. abortus* strains, wild type, CtrA depletion (with or without IPTG) and Δ*virB*, were used to infect HeLa cells. At 10 h PI, cells were fixed and immunofluorescence (IF) was performed to detect bacteria and Lamp1. The proportion of Lamp1+ BCV is shown for each strain/condition. The mean of three independent infections is indicated, the error bars correspond to standard deviation.
B. The CtrA depletion strain was used to infect HeLa cells for 10–24 h (three samples) in the absence of IPTG and IF was performed to detect bacteria and the ER marker Sec61β. The abnormal morphology indicates that bacteria experienced a CtrA depletion inside host cells. The average and standard deviation are shown (497 normal and 153 abnormal bacteria were counted in total).
C. The CtrA depletion strain was used to infect HeLa cells for 15 h (three samples) in the absence of IPTG and immunofluorescence was applied to detect the proportion of ER-associated bacteria using the dolichol kinase (DolK) marker. The average and standard deviation are shown (235 normal and 65 abnormal bacteria were counted in total).

We also investigated the intracellular trafficking of the CtrA depletion strain by monitoring the labeling of BCV with Lamp1, a marker of late endosomes and lysosomes that is excluded from the BCV during a normal trafficking in HeLa cells. Therefore, to test the ability of the CtrA depletion strain to leave Lamp1+ compartments, we chose to monitor the Lamp1 labeling of BCV with this marker at a time PI (10 h), when the WT strain is expected to leave late endosomes (Pizarro-Cerda *et al.*, 1998b; Deghelt *et al.*, 2014). As a control, we used a Δ*virB* strain known to stay in Lamp1+ compartments for up to 12 h PI (Comerci *et al.*, 2001; Celli *et al.*, 2003). Our results showed indeed a low proportion of Lamp1+ vacuoles for the WT strain compared with Δ*virB* ($p < 0.01$) (Fig. 6A and B). The CtrA depletion strain supplemented or not with IPTG had a similar proportion of Lamp1+ vacuoles compared with the WT (Fig 6A), suggesting that its intracellular trafficking is similar to the WT. This suggested that CtrA depletion does not profoundly affect trafficking of *B. abortus* in HeLa cells. Since an abnormal morphology seems to be a typical feature of CtrA depletion (Fig. 2), we evaluated the proportion of bacteria with abnormal morphology in ER compartments, compared with the proportion of bacteria with a normal morphology in the same compartment. To label the ER, we chose two markers, the translocon component Sec61β (Fig. 6B) (Hartmann *et al.*, 1994) and the dolichol kinase (DolK, Fig. 6C) (Shridas and Waechter, 2006), typical proteins of the endoplasmic reticulum. The HeLa cells were infected with the CtrA depletion strain in the absence of IPTG, Sec61β positive (Sec61β+) and DolK positive (DolK+) BCVs were detected using immunofluorescence, and the proportion of Sec61β+ and DolK+ BCVs was evaluated for normal and abnormal morphologies (Fig. 6B and C). If CtrA depletion affects trafficking, one could expect a lower proportion of abnormal morphologies in the ER compartments. Actually, we found that the proportion of Sec61β+ or DolK+ BCVs containing abnormal morphologies was slightly higher compared with the Sec61β+ or DolK + BCV containing bacteria with a normal morphology. The main interpretation of these data is that CtrA depletion does not impair trafficking to the ER. The lower proportion of bacteria with a normal morphology could be explained by the presence of dead or non-growing bacteria, unable to traffic until ER compartments.

CtrA depletion affects OMP amounts

One surprising feature of the CtrA regulon, according to ChIP-seq data (Supporting Information Table S1), is the

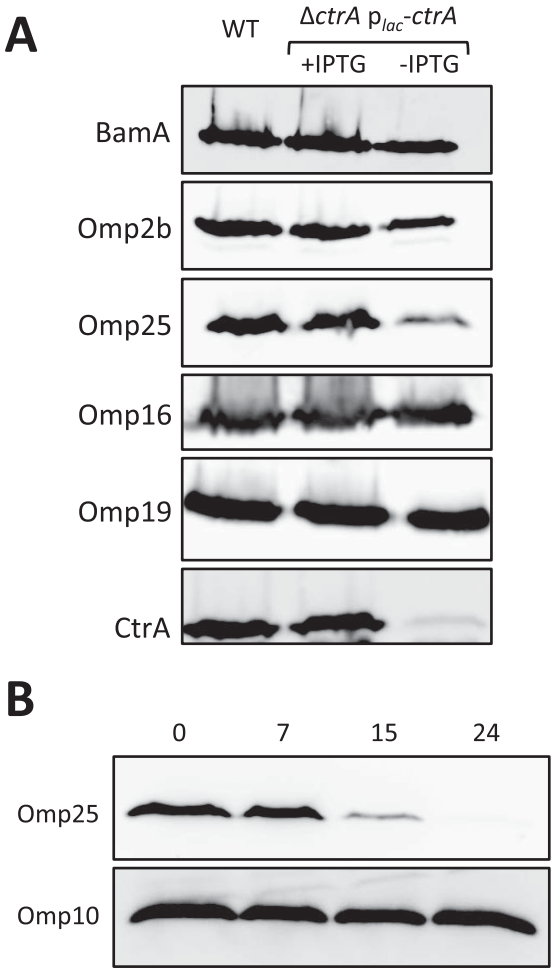

Fig. 7. Effect of the CtrA depletion on outer membrane proteins abundance.
A. Western blots on *B. abortus* lysates of the wild type (WT) strain and the CtrA depletion strain grown with or without IPTG for one night, using monoclonal antibodies recognizing OMPs whose genes were identified by ChIP-seq as being potentially regulated by CtrA.
B. Western blots on lysates of the CtrA depletion strain grown without IPTG for 0, 7, 15, and 24 h, using a monoclonal anti-Omp25 antibody (A68/4B10/F05). Omp10 was detected by Western blot as a loading control.

high proportion of direct targets corresponding to genes encoding outer membrane components, particularly outer membrane proteins (OMPs). To reveal a possible impact of CtrA depletion on the abundance of some of these OMPs, three integral OMPs (Omp2b, Omp25, and BamA) and two proposed OM lipoproteins (Omp16 and Omp19) were detected by Western blot on a *B. abortus* wild type strain, on the CtrA depletion strain cultivated with IPTG and on the same strain depleted in CtrA overnight. While the amount of Omp16 and Omp19 seems to remain unchanged in the absence of CtrA, a slight decrease in the amount of Omp2b and BamA was observed (Fig. 7A). Omp25 abundance was lower in the absence of CtrA, and strongly decreased at longer depletion times (Fig. 7B). Given that OMPs of groups 2 and 3 (Omp2b and Omp25) are the major OMPs in *Brucella* envelope (Dubray and Charriaut, 1983), their reduced abundance in the absence of CtrA could lead to the perturbation of the envelope, which could have dramatic consequences for the bacterium when it is inside host cells (Fig. 3C).

We also labeled Omp25 present at the surface of *B. abortus* by immunofluorescence. The localization of Omp25 on the CtrA-depletion strain grown overnight without IPTG was heterogeneous. This was observed with a monoclonal antibody directed against Omp25 (Supporting Information Fig. S8). The labeling was often partial and concentrated on the tip of the branches (Fig. 8A). For the wild type strain, 86.6% of the bacteria were either completely unlabeled or displayed an homogeneous labeling (Fig. 8B). The Δ*ctrA* p$_{lac}$-*ctrA* depletion strain cultivated in the presence of IPTG displayed a similar proportion of unlabeled or homogeneously labeled bacteria (82.2%) (Supporting Information Fig. S8). Partially labeled bacteria were counted in three independent experiments, and their proportion is reported in Fig. 8C. The proportion of partially labeled bacteria was significantly higher for the depletion strain compared with the wild type strain ($p < 2.1\ 10^{-5}$ in a Scheffé statistical analysis). These data suggest that in the absence of CtrA, Omp25 localization on the surface of *B. abortus* is perturbed. Curiously, the Omp25 labeling pattern was symmetric, meaning that if the tip of one branch is labeled, the tip of the other branches is also labeled (Fig. 8A). One plausible explanation is that Omp25 is incorporated in the outer membrane in a similar manner in all parts of the branched cells that are generated at the same time. In this model, Omp25 proteins remain immobile in the outer membrane, probably because they are directly or indirectly bound to peptidoglycan (Cloeckaert *et al.*, 1992).

Discussion

The essential transcription factor CtrA is known to be at the heart of a complex network regulating the cell cycle progression of the model organism *C. crescentus*. CtrA is essential and its regulon is also partially conserved in *S. meliloti* (Pini *et al.*, 2015). However, in phylogenetically more distant organisms such as *Rhodospirillales* (Greene *et al.*, 2012) or *Rhodobacterales*, CtrA is not essential and has evolved to regulate cell cycle-independent processes (Lang and Beatty, 2000; Cheng *et al.*, 2011; Mercer *et al.*, 2012; Francez-Charlot *et al.*, 2015). Analysis of the expression of CtrA targets in *B. abortus* suggests that CtrA is involved in cell cycle-dependent regulation (Fig. 4).

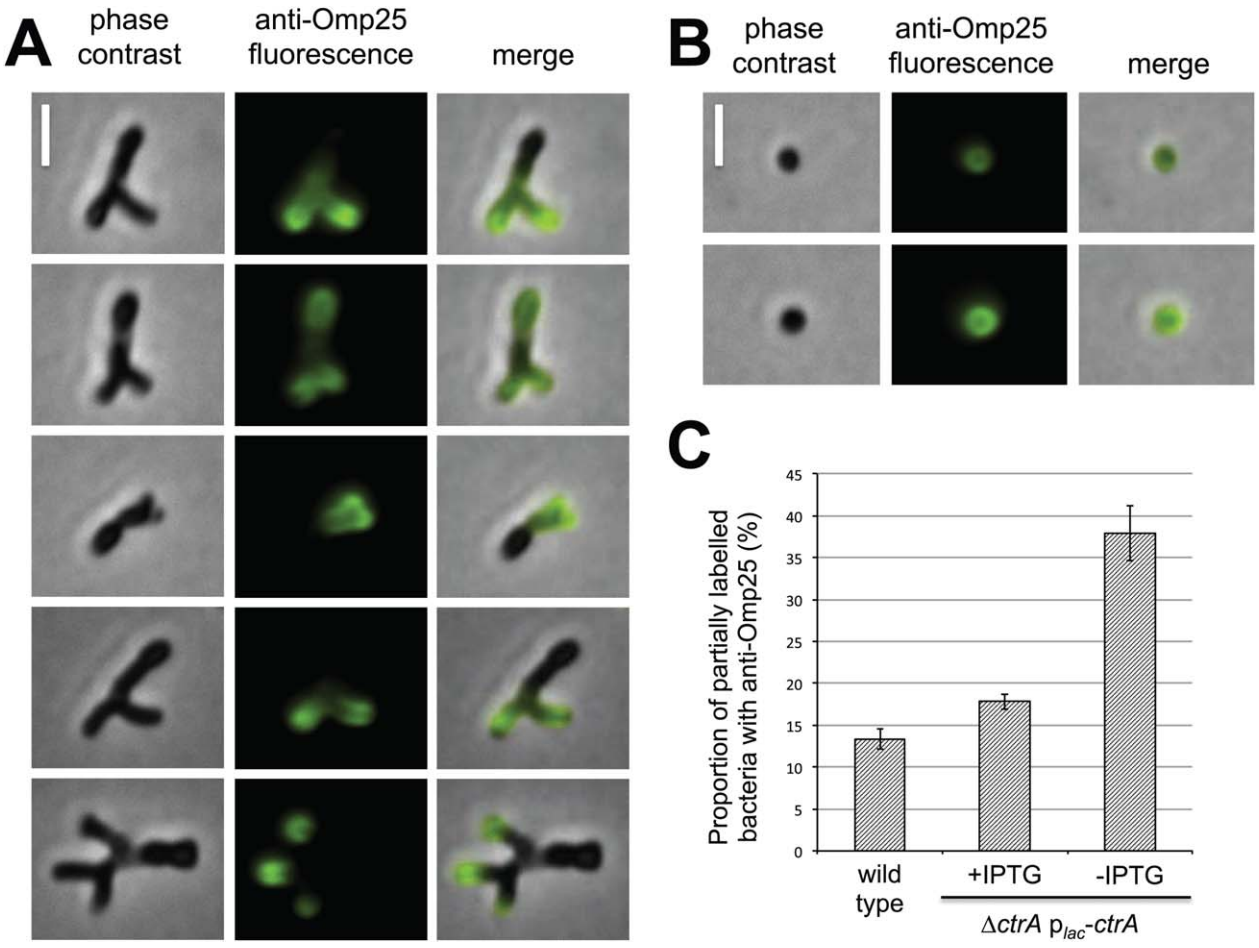

Fig. 8. Effect of CtrA depletion on Omp25 localization.
A. Phase contrast microscopy and associated fluorescent anti-Omp25 signal of the CtrA depletion strain cultivated in the absence of IPTG. In these bacteria, the Omp25 signal is localized at the tip of the branches, revealing the heterogeneity of the outer membrane composition in these bacteria. These localization patterns also suggest that Omp25 diffusion in the outer membrane is slow.
B. Homogeneous localization of anti-Omp25 signal on the wild type strain. The scale bars correspond to 2 μm.
C. Proportion of partially labeled bacteria generated with the anti-Omp25 antibody, for the wild type strain or the depletion strain cultivated in the presence or in absence of IPTG. Standard deviations are shown ($n = 3$).

Here, we show that CtrA regulon in *B. abortus* is partially conserved in comparison with *C. crescentus* and *S. meliloti* CtrA regulons. They indeed share genes involved in cell cycle regulation such as DNA methylation, chromosome replication, and segregation and division (Laub *et al.*, 2002; Pini *et al.*, 2015). However, as previously suggested by the identification of a limited number of CtrA targets in *B. abortus* (Bellefontaine *et al.*, 2002), a similar process can be regulated through different target genes. For example, CtrA is binding to the *mipZ* promoter in *C. crescentus* (Fumeaux *et al.*, 2014), allowing the control of Z ring positioning, while this control is proposed to be mediated by the binding to the *minCDE* promoter in *B. abortus* (Bellefontaine *et al.*, 2002), as also recently elucidated in *S. meliloti* (Pini *et al.*, 2015). These comparisons underline the plasticity of the CtrA regulon along evolution.

Depletion of CtrA leads to a severe (Fig. 2) and reversible (Supporting Information Fig. S4) cell division defect in *B. abortus*. However, among the direct targets of CtrA found in the conditions tested here, cell cycle-related genes are not restricted to cell division. Indeed, genes involved in replication, the DivK-CtrA regulation network and the recruitment of proteins to the poles (*popZ*) have also their promoter enriched by ChIP-seq. Besides cell cycle-related genes, one obvious conclusion of the ChIP-seq experiment reported here is the high proportion of genes involved in envelope biogenesis or homeostasis. Indeed, CtrA predicted regulon is enriched in genes coding for LPS and outer membrane proteins biosynthesis and export. The presence of CtrA is crucial for the production of normal amounts of Omp25 (Fig. 7) and for an homogeneous distribution of Omp25 on the surface of the bacterium (Fig. 8). We

cannot exclude that alteration of Omp25 localization on the surface is an indirect effect of the inhibition of cell division. Indeed it is likely that the generation of elongated and branched morphologies takes more time than the generation of normal shaped bacteria, thus partially labeled bacteria could reveal the oscillating nature of Omp25 incorporation in the outer membrane in these cells. A *B. abortus* deletion strain for *omp25* was found to be attenuated in cattle (Edmonds *et al*., 2001), but more recent data suggested that this attenuation could be explained by a higher internalization and a higher intracellular killing of the *omp25* mutant compared with the wild type strain (Manterola *et al*., 2007). The molecular functions of the highly abundant Omp25 are still unknown; it was shown to inhibit TNFα production in human macrophages (Jubier-Maurin *et al*., 2001) and it could be involved in defining the properties of the outer membrane by interacting with the LPS (Manterola *et al*., 2005). Interestingly, in *S. meliloti*, CtrA binds to the promoter of *ropB* gene (Pini *et al*., 2015), encoding an Omp25 homolog involved in outer membrane stability in *Rhizobium leguminosarum* (Vanderlinde and Yost, 2012). It is thus possible that in *Rhizobiales*, CtrA controls factors involved in outer membrane biogenesis or homeostasis. Their control by CtrA would have been acquired after the divergence from the common ancestor with *C. crescentus*, since CtrA regulon of *C. crescentus* is not particularly enriched in genes involved in outer membrane biogenesis or homeostasis (Laub *et al*., 2002; Fumeaux *et al*., 2014).

Depletion of CtrA results in a strong inhibition of cell division (Fig. 2A), possibly explaining why the *ctrA* gene is essential in *B. abortus* as suggested in previous studies (Bellefontaine *et al*., 2002; Willett *et al*., 2015). The inhibition of cell division results in branched morphology or formation of small chains of cells, the latter being probably produced by incomplete septation. It is noteworthy that the CtrA-loss of function phenotype is reversible, as induction of *ctrA* expression after depletion resulted in the reactivation of cell division (Supporting Information Fig. S4). Perturbation of division in the CtrA-depleted condition is likely explained by the presence of numerous genes and operons involved in division in the CtrA predicted regulon. Indeed, the *minCDE* operon is involved in Z ring placement, and many genes and operons proposed to be involved in the cell division process, like *ftsQAZ*, *ftsEX*, *ftsK*, and the *pal(omp16)-tolQRAB* locus are detected as possible direct targets of CtrA in *B. abortus* (Supporting Information Table S1). The deregulation of some of these genes is probably sufficient to block the whole cell division process.

Depletion of CtrA also resulted in altered morphology of bacteria infecting host cells (Fig. 5B). During infection elongated and branched morphologies can only be generated by growth, suggesting that these bacteria are able to uptake nutrients during cellular infection, after an initial stage of growth arrest that could be due to starvation (see below). In host cells, the timing of the appearance of the altered morphologies is different from the timing of their formation in bacteriological medium. Indeed, in HeLa cells abnormal morphologies of the CtrA depletion strain appeared around or after 10 h PI (Fig. 5B), mainly consisting of elongated cells (Fig. 5A) resembling bacteria recovered 3 h after IPTG removal in rich culture medium (Fig. 2A). At 15 h PI, branched bacteria were observed (Fig. 5A), similarly to the 7 h depletion in culture (Fig. 2A). Interestingly, *B. abortus* was shown to resume its intracellular growth around 8 h PI in HeLa cells (Deghelt *et al*., 2014). The observation of elongated bacteria at or after 10 h PI for the CtrA-depleted bacteria thus suggests that the absence of CtrA does not drastically change the timing of growth arrest/resumption in HeLa cells. If CtrA is not required for the control of the intracellular growth arrest/resumption, it is likely that other regulation networks, like those triggered by starvation (Dozot *et al*., 2006), could be involved. Previous work also showed that *B. abortus* growth is resumed in Lamp1+ compartments around 8 h PI and that daughter cells are found almost exclusively in Lamp1- compartment from 10 h PI (Deghelt *et al*., 2014). While CtrA depleted bacteria with a normal morphology could be dead or non-growing bacteria unable to traffic until the ER, bacteria that have grown to generate branching morphology are able to traffic to the ER, demonstrating that they are able to perform this crucial step of intracellular trafficking. This suggests that despite their morphological alterations, these bacteria are probably still able to produce a functional VirB system, which is required for this step of their intracellular trafficking (Comerci *et al*., 2001; Delrue *et al*., 2001). Thus CtrA-dependent cell cycle control and intracellular trafficking seem to be relatively independent processes in *B. abortus*. The dramatic drop of the CFU counts at 48 h PI (Fig. 3B) suggests that the branched bacteria are unable to survive for long periods in host cells.

In conclusion, our data support the idea that along evolution of the CtrA regulon, CtrA has kept the control of cell division in many *Alphaproteobacteria*. However, in *B. abortus* and possibly in *Rhizobiales* it also acquired new functions, including the control of envelope composition. It is interesting to realize that CtrA has to be cleared from *S. meliloti* cells to allow them to differentiate into nitrogen-fixing bacteroids inside host plants (Pini *et al*., 2013), illustrating that fundamental processes of bacterial cell cycle have been adapted to the lifestyle of pathogens and symbionts within the *Alphaproteobacteria*.

Experimental procedures

Bacterial strains and media

E. coli strains DH10B, BL21 (DE3) and DB3.1 were grown in Luria-Bertani (LB) medium at 37°C. Derivatives of the *B. abortus* 544 Nal^R strain were cultivated in 2YT rich medium (1% yeast extract, 1.6% peptone, 0.5% NaCl) at 37°C. Antibiotic concentrations are the following: ampicillin, 100 μg/ml; kanamycin, 20 or 50 μg/ml; chloramphenicol, 20 μg/ml; nalidixic acid, 25 μg/ml; rifampicin, 20 μg/ml; gentamicin, 50 μg/ml. *B. abortus* strains were constructed as previously described (Deghelt *et al.*, 2014). Plasmids are listed in Supporting Information Table S2.

Cloning of the pBBR-MCS1-p_{lacI}-lacI-p_{lac}-ctrA

The p_{lacI}-*lacI*-p_{lac} sequence was amplified from the pSRK-Kan vector (Khan *et al.*, 2008) using Phusion High-Fidelity DNA Polymerase (New England BioLabs) and *Sac*I-Kan3' and p_{lac}-R1 primers (see Supporting Information Table S3). The *ctrA* coding sequence was amplified from *B. abortus* 544 purified genomic DNA using *ctrA*-F2 and *Kpn*I-*ctrA*-R2 primers. The PCR product was fused to the p_{lacI}-*lacI*-p_{lac} sequence by joining PCR. The p_{lacI}-*lacI*-p_{lac}-*ctrA* insert was then cloned in the pBBRMCS1 using *Sac*I and *Kpn*I restriction enzymes. By using these enzymes, the insert was cloned in the opposite orientation to the p_{lac} promoter of the pBBRMCS1.

Cloning of a ctrA deletion for allelic exchange

The *ctrA* gene was deleted from *B. abortus* 544 chromosome by allelic replacement. A 750 base pair (bp)-region upstream and another one downstream of *ctrA* were amplified by PCR using *Pst*I-Up-*ctrA*-F/Up-*ctrA*-R and Down-*ctrA*-F/*Sal*I-Down-*ctrA*-R pairs of primers respectively and both PCR products were fused together by joining PCR. The PCR product was cloned in the pNPTS138 vector (M. R. K. Alley, Imperial College of Science, London, UK) carrying a kanamycin resistance cassette and a sucrose sensitivity cassette.

Cloning of reporter vectors

Promoter regions were amplified from *B. abortus* 544 purified genomic DNA using Phusion High-Fidelity DNA Polymerase and fused by joining PCR to *gfp*(ASV). The pairs of primers used to amplify the promoter regions are *Xba*I-p_{ctrA}-F1/p_{ctrA}-R1, *Xba*I-p_{repAB}-F1/p_{repAB}-R1, *Xba*I-p_{ccrM}-F1/p_{ccrM}-R1 and *Xba*I-p_{pleC}-F1/p_{pleC}-R1. The pair of primers used to amplify the *gfp*(ASV) gene is *gfP*(ASV)-F2/*Xho*I-*gfp*(ASV)-R2. *Xba*I and *Xho*I restriction sites were added to the upstream and downstream primers. The fusion was first cloned in pGEMT digested by *Eco*RV, generating blunt ends, and sequenced. A *Xba*I-*Xho*I restriction allowed the transfer of the insert to a pBBRMCS1 vector, in the opposite direction to the *lac* promoter of the vector.

Mutagenesis of the CtrA boxes was generated in the same way, but using the constructs with a wild type promoter as DNA template. The *Xba*I-p_{gene}-F1 and *Xho*I-*gfp*(ASV)-R2 were kept as they were but their corresponding pair of primer (R1 and F2) were modified to include the mutated CtrA-binding boxes. In the case of p_{ccrM}-mut1&2-*gfp*(ASV), boxes were mutated sequentially (CtrA-binding box 1, followed by CtrA-binding box 2). The wild type and mutated promoters are shown in Supporting Information Fig S5.

Chromatin immunoprecipitation with anti-CtrA antibodies

An 80 ml culture of *B. abortus* 544 at an OD_{600} of 0.8 was centrifuged to harvest the bacteria. Protein-DNA crosslinking was performed in 10 μM sodium phosphate buffer (pH 7.6) and 1% formaldehyde for 10 min at RT and 30 min on ice. Bacteria were harvested by centrifugation at 8500 rpm for 5 min at 4°C, washed twice in cold PBS and resuspended in lysis buffer (10 mM Tris-HCl pH 7.5, 1 mM EDTA, 100 mM NaCl, 2.2 mg/ml lysozyme, 20 μl protease inhibitor solution). Zirconia/Silica beads (Biospec Products) of 0.1 and 0.5 mm diameter were added. Bacteria were lysed in the cell Disruptor Genie from Scientific Industries at maximal amplitude (2800) for 25 min at 4°C. ChIP buffer was added (1.1% TritonX-100, 1.2 mM EDTA, 16.7 mM Tris-HCl pH 8.0, 167 mM NaCl, protease inhibitors) and bacteria were incubated at 37°C for 10 min for further lysis. The lysate was sonicated on ice (Branson Sonifier Digital cell disruptor S-450D 400W) by applying 15 bursts of 20 s (50% duty) at 30% amplitude to cut the DNA to fragments of about 300 base pairs and centrifuged at 14,000 rpm for 3 min to pellet the debris. The supernatant was normalized by protein content by measuring the absorbance at 280 nm. Around 7.5 mg of protein was diluted in 1 ml of ChIP buffer supplemented with 0.01% SDS and pre-cleared in 80 μl of protein A-agarose beads (Roche) and 100 μg BSA. Polyclonal anti-CtrA antibodies (Bellefontaine *et al.*, 2002) were added to the supernatant (dilution 1:1000) and incubated for one night at 4°C to form immune complexes which were then incubated with 80 μl of protein A-agarose beads pre-saturated with BSA for 2 h at 4°C. Beads were then washed once with low salt buffer (0.1% SDS, 1% TritonX-100, 2 mM EDTA, 20 mM Tris-HCl pH 8.1, 150 mM NaCl), high salt buffer (0.1% SDS, 1% TritonX-100, 2 mM EDTA, 20 mM Tris-HCl pH 8.1, 500 mM NaCl) and LiCl buffer (0.25 M LiCl, 1% NP-40, 1% sodum deoxycholate, 1 mM EDTA, 10 mM Tris-HCl pH 8.1) and twice with TE buffer (10 mM Tris-HCl pH 8.1 and 1 mM EDTA). Protein-DNA complexes were eluted with 500 μl of elution buffer (1% SDS and 0.1M $NaHCO_3$). Reverse crosslinking was performed in presence of 300 mM of NaCl O/N at 65°C. Samples were treated with 2 μg of Proteinase K for 2h at 45°C in 40 mM EDTA and 40 mM Tris-HCl pH 6.5. DNA was extracted using QIAgen minelute kit and resuspended in 30 μl of Elution Buffer. ChIP DNA was sequenced using Illumina MySeq.

Analysis of the sequencing data

Sequencing data consisted of a number of reads per nucleotide. Computing of average and variance in a window of 1

million base pairs allowed the calculation of *Z* score pour each base pair (i.e., the number of standard deviation from the average). Genomic regions with reads numbers above the threshold ($Z > 4$) were kept and considered to be bound by CtrA. These regions were mapped to the genome of *B. abortus* 2308, a close relative to the *B. abortus* 544 strain. The mapping is available in the Supplemental files ChIP-seq_CtrA_chr1.txt and ChIP-seq_CtrA_chr2.txt, that can be analyzed using the Chr1.gb and Chr2.gb genomic sequences respectively, with the Artemis program (freely available at the following website http://www.sanger.ac.uk/science/tools/artemis).

Electrophoretic mobility shift assay

DNA probes of 50–70 pb were prepared by amplifying promoter regions from *B. abortus* 544 purified genomic DNA using Phusion High Fidelity DNA Polymerase (see Supporting Information Table S3 for list of primers, named as EMSA-F/R-promoter). Each PCR product was concentrated and purified after migration on agarose gel electrophoresis, using NucleoSpin® Gel and PCR Clean-up (Macherey-Nagel) according to manufacturer's instructions. These purified PCR products were then used as template for a new amplification with a cyanine-5(Cy5)-labeled primer (Integrated DNA Technologies) (Supporting Information Table S3). The labeled amplicons were purified after gel electrophoresis and quantified using a Qubit® 3.0 Fluorometer (Thermo Fisher Scientific).

His_6-CtrA was purified and phosphorylated as previously described (Bellefontaine *et al.*, 2002). Binding reactions were prepared in a final volume of 20 μl with 0–340 μg of CtrA, 3 ng of labeled probes and when necessary with 400 ng of competing probe (non-labeled PCR product) in binding buffer (10 mM Tris pH 7.4, 10 mM $MgCl_2$, 50 mM NaCl, 10% glycerol). Samples were incubated for 30–45 min at 37°C and 10 μl were loaded onto a 13.3% polyacrylamide gel (3.9 ml of ddH_2O, 700 μl of 5X TBE buffer, 2.3 ml of 40% acrylamide stock 19:1, 70 μl of 10% APS and 7 μl of TEMED). TBE is 89 mM Tris, 89 mM boric acid and 2 mM EDTA, pH 8.3. Samples were run at 100V for 3h20 in 0.5 × TBE buffer at 4°C. Samples were revealed using an Amersham Imager 600 (GE Healthcare Life Sciences) with the Cy5 fluorescence channel.

Reverse transcription followed by quantitative PCR

The *B. abortus* strains were grown in rich medium (2YT) until exponential phase, washed and growth was restart in rich medium, with or without IPTG for 6 h. Then bacteria were washed in PBS, collected by centrifugation and immediately frozen and stored at −80°C until processing. RNA was then extracted with TriPure isolation reagent (Roche) according to the instructions of the manufacturer. DNA contamination was eliminated by incubation with DNase I (Fermentas). RNA was reverse transcribed with specific primers, using the High capacity cDNA Reverse Transcription kit (Applied Biosystems). Specific cDNAs were amplified using FastStart Universal SYBR Green Master (Roche) with a LightCycler 96 Instrument (Roche). The specificity of the PCR was assessed by melting-point analysis and gel electrophoresis. Results were normalized using the housekeeping *groEL* gene as a reference. Primer sequences (with a name starting by RT-qPCR) are available in Supporting Information Table S3.

TRSE labeling

Bacteria were harvested by centrifugation at 7000 rpm for 2 min. They were then washed thrice with phosphate-buffered saline (PBS) and incubated with Texas Red succinimidyl ester (TRSE) from Invitrogen diluted at 1 μg/ml in PBS for 15 min at room temperature (RT) in the dark. Bacteria were then washed once with PBS and twice with the appropriate medium, 2YT for growth assays and Dulbecco's Modified Eagle's Medium (DMEM) for HeLa cells infections.

Microscopy and analysis of GFP fluorescence in the reporter systems using MicrobeTracker

Brucella abortus strains labeled with TRSE were analyzed by fluorescence microscopy as previously reported (Deghelt *et al.*, 2014). The pairwise comparisons of the proportions of morphotypes such as elongated cells or bacteria with mislocalized constriction sites were made using a Scheffe analysis. *B. abortus* strains expressing a promoter-*gfp* fusion were observed using a Nikon 80i (objective phase contrast ×100, plan Apo) connected to a Hamamatsu ORCA-ER camera. Cell meshes were obtained using the Matlab-based MicrobeTracker software (Sliusarenko *et al.*, 2011), determining the cell length and quantifying the average amount of fluorescence per bacterium. Data were then transferred to Excel files using the "XLStotmeansteparea.m" script. Data were sorted according to bacterial cell length, and the mean cell length and mean fluorescence intensity were calculated using a sliding window of 300 bacteria.

HeLa cells culture and infection

HeLa cells (from the Centre d'Immunologie de Marseille-Luminy, Marseille, France) were cultivated at 37°C and in a 5% CO_2 atmosphere in DMEM (Invitrogen) supplemented with 10% fetal bovine serum (Gibco), 0.1 g/l non-essential amino acids and 0.1 g/l sodium pyruvate (Invitrogen). For the infection, HeLa cells were seeded in 24-well plates (on coverslips for immunolabeling) at a concentration of 4.10^4 cells/ml. On the day of the infection, an O/N culture of *B. abortus* was diluted in DMEM to reach an MOI (multiplicity of infection) of 300. Bacteria were added to HeLa cells and the 24-well plates were centrifuged at 1200 rpm for 10 min at 4°C. Cells were then incubated at 37°C in a 5% CO_2 atmosphere for 1 h. Cells were washed twice in PBS and fresh medium supplemented with 50 μg/ml gentamicin was added.

Immunolabeling of infected HeLa cells

Cells were fixed in PBS 2% paraformaldehyde (Prolabo) for 20 min at RT then permeabilized in PBS 0.1% Triton X-100 for 10 min. Cells were incubated for 45 min with primary

and secondary antibodies supplemented with 0.1% Triton X-100 and 3% bovine serum albumin (BSA, Sigma Aldrich). *Brucella* were detected with the A76-12G12 monoclonal antibody (non-diluted hybridoma culture supernatant) followed by a secondary anti-mouse antibodies coupled to Alexa-488 diluted 500 times (Sigma Aldrich). Coverslips were washed thrice with PBS and once with $_{dd}H_2O$ and mounted with Mowiol (Sigma). Antibodies are listed in Supporting Information Table S4.

For Lamp1 labeling, cells were fixed in methanol-acetone (80%-20%) for 20 min at RT. Bacteria and Lamp1 were labeled with a rabbit anti-*Brucella* serum diluted 2000 times and mouse anti-Lamp1 antibodies diluted 200 times in PBS 2% BSA. Secondary anti-rabbit antibodies coupled to Pacific Blue and anti-mouse antibodies coupled to Alexa-488 (Sigma Aldrich) were diluted 500 times in PBS 2% BSA. Coverslips were washed thrice in PBS 2% BSA and mounted with Mowiol. For each strain in each condition (± IPTG), the number of BCVs analyzed was as follows: 66–77 for the wild type strain, 62–100 for the depletion strain with IPTG, 48–70 for the depletion strain without IPTG, and 36–71 for the Δ*virB* strain.

For endoplasmic reticulum (ER) labeling, cells were fixed in PBS 2% paraformaldehyde for 20 min at RT, then washed twice with PBS before to be permeabilized with PBS 0.2% saponin (Sigma Aldrich) for 20 min at RT. Cells were then blocked for 30 min with 0.2% saponin, 3% BSA, 50 mM NH_4Cl in 0.1% dPBS-Tween20. ER was labeled either with primary anti-DOLK rabbit antibody (Abcam, ab93609) diluted 200 times or with anti-Sec61β rabbit antibody (B. Dobberstein, Universität Heidelberg, Heidelberg, Germany) diluted 100 times, both in 3% BSA, 0.2% saponin and 0.1% dPBS-Tween20. Secondary anti-rabbit coupled to Alexa-488 (Sigma Aldrich) diluted 500 times were used for staining after washing thrice with PBS. *B. abortus* were labeled using non-diluted A76-12G12 primary antibody obtained from homemade hybridoma culture supernatant in 0.2% saponin and 3% BSA, followed by a secondary anti-mouse antibody coupled to TxRed (Sigma Aldrich) diluted 500 times in 3% BSA, 0.2% saponin and 0.1% dPBS-Tween20. Coverslips were washed thrice in PBS and once in ddH2O before to be mounted on Mowiol. The infections were repeated three times independently, and 167–317 BCVs were analyzed in each infection.

Growth curve and CFU counts

Growth curves were performed by using Bioscreen C from Oy Growth curves. O/N cultures were diluted to an OD of 0.1 and the OD was measured every 30 min during 70 h. For CFU counts in culture, wild type (WT) *B. abortus* 544 and the CtrA depletion strain supplemented with IPTG were diluted to 10^{-6} or 10^{-7} in 2YT and 100 µl were plated on 2YT, supplemented with chloramphenicol and 1 mM IPTG for the depletion strain. The depletion strain grown without IPTG was diluted to 10^{-4} or 10^{-5}. For CFU counts after infection, HeLa cells were lysed with 0.01% TritonX-100 PBS for 10 min at RT. Several dilutions were plated on 2YT supplemented with chloramphenicol and IPTG if needed. Plates were incubated for 3–4 days at 37°C.

Western blot analysis

One milliliter of a *B. abortus* culture was concentrated to an OD_{600} of 10 in PBS. Bacteria were inactivated for 1 h at 80°C and loading buffer was added. Fifteen µl of bacterial lysate was loaded in each well. After migration, proteins were transferred onto a nitrocellulose membrane which was blocked in PBS supplemented with 0.05% Tween and 5% milk for at least 1 h. The membrane was incubated for 1 h with the appropriate serum (diluted 10, 100, or 1000× depending on the serum) and secondary antibodies coupled to HRP (diluted 5000×) (Dako Denmark) diluted in PBS 0.05% Tween 1% milk. The membrane was washed for 3 times for 5 min. The Clarity Western ECL Substrate (Biorad) and Image Quant LAS 4000 (General Electric) were used to reveal the bands.

Immunodetection of Omp25 on bacteria

Bacteria grown overnight in rich culture medium were washed twice in PBS by centrifugation at 4000 rpm for 2.5 min and resuspension. Washed bacteria were resuspended in non-diluted hybridoma culture supernatant containing monoclonal anti-Omp25 antibodies and secondary anti-mouse antibodies coupled to Alexa-488 diluted 500 times in PBS, and were incubated for 40 min at RT on a wheel. Bacteria were washed twice in PBS and 2 µl were dropped on an agarose pad (1% PBS agarose) for microscopy.

Acknowledgements

We thank Véronique Dhennin from the UMR8199 sequencing service LIGAN-PM Equipex (Lille Integrated Genomics Advanced Network for personalized medicine) and Aurélie Mayard for assistance in protein purification and Western blotting. This research has been funded by the Interuniversity Attraction Poles Programme initiated by the Belgian Science Policy Office (https://www.belspo.be/) to J.-J. Letesson and by grants from Fonds de la Recherche Scientifique-Fonds National de la Recherche Scientifique (FRS-FNRS, http://www.fnrs.be) (PDR T.0053.13 and PDR Brucell-cycle T.0060.15, CDR J.0091.14 and FRFC 2.4.541.08 F) to X. De Bolle. We thank UNamur (https://www.unamur.be/) for financial and logistic supports. This work was supported by the French Agence Nationale de Recherche (ANR-JCJC-2011-Castacc) (http://www.agence-nationale-recherche.fr/) and the Region Pas-De-Calais (http://www.nordpasdecalais.fr) CPER to A. Fioravanti and Emanuele G. Biondi. N. Francis held an Aspirant fellowship from FRS-FNRS. K. Poncin and V. Vassen are supported by a Ph.D. grant from FRIA (FRS-FNRS). The authors declare no conflict of interest.

Author contributions

NF, KP, AV, VV, KW, TAPO, and LR acquired and analyzed the data; NF, JJL, EB, and XDB designed the study; NF, JJL, EB, and XDB wrote the manuscript.

References

Andersen, J.B., Sternberg, C., Poulsen, L.K., Bjorn, S.P., Givskov, M., and Molin, S. (1998) New unstable variants of green fluorescent protein for studies of transient gene expression in bacteria. *Appl Environ Microbiol* **64**: 2240–2246.

Anderson, E.S., Paulley, J.T., Gaines, J.M., Valderas, M.W., Martin, D.W., Menscher, E., Brown, *et al*. (2009) The manganese transporter MntH is a critical virulence determinant for *Brucella abortus* 2308 in experimentally infected mice. *Infect Immun* **77**: 3466–3474.

Archambaud, C., Salcedo, S.P., Lelouard, H., Devilard, E., de Bovis, B., Van Rooijen, N., *et al*. (2010) Contrasting roles of macrophages and dendritic cells in controlling initial pulmonary *Brucella* infection. *Eur J Immunol* **40**: 3458–3471.

Bellefontaine, A.F., Pierreux, C.E., Mertens, P., Vandenhaute, J., Letesson, J.J., and De Bolle, X. (2002) Plasticity of a transcriptional regulation network among alpha-proteobacteria is supported by the identification of CtrA targets in *Brucella abortus*. *Mol Microbiol* **43**: 945–960.

Brilli, M., Fondi, M., Fani, R., Mengoni, A., Ferri, L., Bazzicalupo, M., and Biondi, E.G. (2010) The diversity and evolution of cell cycle regulation in alpha-proteobacteria: a comparative genomic analysis. *BMC Syst Biol* **4**: 52.

Brown, P.J., de Pedro, M.A., Kysela, D.T., Van der Henst, C., Kim, J., De Bolle, X., *et al*. (2012) Polar growth in the Alphaproteobacterial order Rhizobiales. *Proc Natl Acad Sci USA* **109**: 1697–1701.

Celli, J., de Chastellier, C., Franchini, D.M., Pizarro-Cerda, J., Moreno, E., and Gorvel, J.P. (2003) Brucella evades macrophage killing via VirB-dependent sustained interactions with the endoplasmic reticulum. *J Exp Med* **198**: 545–556.

Celli, J., Salcedo, S.P., and Gorvel, J.P. (2005) *Brucella* coopts the small GTPase Sar1 for intracellular replication. *Proc Natl Acad Sci USA* **102**: 1673–1678.

Chaves-Olarte, E., Guzman-Verri, C., Meresse, S., Desjardins, M., Pizarro-Cerda, J., Badilla, J., *et al*. (2002) Activation of Rho and Rab GTPases dissociates *Brucella abortus* internalization from intracellular trafficking. *Cell Microbiol* **4**: 663–676.

Cheng, Z., Miura, K., Popov, V.L., Kumagai, Y., and Rikihisa, Y. (2011) Insights into the CtrA regulon in development of stress resistance in obligatory intracellular pathogen *Ehrlichia chaffeensis*. *Mol Microbiol* **82**: 1217–1234.

Cloeckaert, A., Zygmunt, M.S., de Wergifosse, P., Dubray, G., and Limet, J.N. (1992) Demonstration of peptidoglycan-associated *Brucella* outer-membrane proteins by use of monoclonal antibodies. *J Gen Microbiol* **138**: 1543–1550.

Comerci, D.J., Martinez-Lorenzo, M.J., Sieira, R., Gorvel, J.P., and Ugalde, R.A. (2001) Essential role of the VirB machinery in the maturation of the *Brucella abortus*-containing vacuole. *Cell Microbiol* **3**: 159–168.

Curtis, P.D., and Brun, Y.V. (2010) Getting in the loop: regulation of development in *Caulobacter crescentus*. *Microbiol Mol Biol Rev* **74**: 13–41.

De Bolle, X., Crosson, S., Matroule, J.Y., and Letesson, J.J. (2015) *Brucella abortus* cell cycle and infection are coordinated. *Trends Microbiol* **23**: 812–821.

Deghelt, M., Mullier, C., Sternon, J.F., Francis, N., Laloux, G., Dotreppe, D., *et al*. (2014) G1-arrested newborn cells are the predominant infectious form of the pathogen *Brucella abortus*. *Nat Commun* **5**: 4366.

Delrue, R.M., Martinez-Lorenzo, M., Lestrate, P., Danese, I., Bielarz, V., Mertens, P., *et al*. (2001) Identification of *Brucella* spp. genes involved in intracellular trafficking. *Cell Microbiol* **3**: 487–497.

Detilleux, P.G., Deyoe, B.L., and Cheville, N.F. (1990) Penetration and intracellular growth of *Brucella abortus* in nonphagocytic cells *in vitro*. *Infect Immun* **58**: 2320–2328.

Domian, I.J., Quon, K.C., and Shapiro, L. (1997) Cell type-specific phosphorylation and proteolysis of a transcriptional regulator controls the G1-to-S transition in a bacterial cell cycle. *Cell* **90**: 415–424.

Dozot, M., Boigegrain, R.A., Delrue, R.M., Hallez, R., Ouahrani-Bettache, S., Danese, I., *et al*. (2006) The stringent response mediator Rsh is required for *Brucella melitensis* and *Brucella suis* virulence, and for expression of the type IV secretion system virB. *Cell Microbiol* **8**: 1791–1802.

Dubray, G., and Charriaut, C. (1983) Evidence of three major polypeptide species and two major polysaccharide species in the Brucella outer membrane. *Ann Vet Res* **14**: 311–318.

Edmonds, M.D., Cloeckaert, A., Booth, N.J., Fulton, W.T., Hagius, S.D., Walker, J.V., and Elzer, P.H. (2001) Attenuation of a *Brucella abortus* mutant lacking a major 25 kDa outer membrane protein in cattle. *Am J Vet Res* **62**: 1461–1466.

Francez-Charlot, A., Kaczmarczyk, A., and Vorholt, J.A. (2015) The branched CcsA/CckA-ChpT-CtrA phosphorelay of *Sphingomonas melonis* controls motility and biofilm formation. *Mol Microbiol* **97**: 47–63.

Fumeaux, C., Radhakrishnan, S.K., Ardissone, S., Theraulaz, L., Frandi, A., Martins, D., *et al*. (2014) Cell cycle transition from S-phase to G1 in Caulobacter is mediated by ancestral virulence regulators. *Nat Commun* **5**: 4081.

Gee, J.M., Valderas, M.W., Kovach, M.E., Grippe, V.K., Robertson, G.T., Ng, W.L., *et al*. (2005) The *Brucella abortus* Cu, Zn superoxide dismutase is required for optimal resistance to oxidative killing by murine macrophages and wild-type virulence in experimentally infected mice. *Infect Immun* **73**: 2873–2880.

Gerding, M.A., Ogata, Y., Pecora, N.D., Niki, H., and de Boer, P.A. (2007) The trans-envelope Tol-Pal complex is part of the cell division machinery and required for proper outer-membrane invagination during cell constriction in E. coli. *Mol Microbiol* **63**: 1008–1025.

Grangeon, R., Zupan, J.R., Anderson-Furgeson, J., and Zambryski, P.C. (2015) PopZ identifies the new pole, and PodJ identifies the old pole during polar growth in *Agrobacterium tumefaciens*. *Proc Natl Acad Sci USA* **112**: 11666–11671.

Greene, S.E., Brilli, M., Biondi, E.G., and Komeili, A. (2012) Analysis of the CtrA pathway in Magnetospirillum reveals an ancestral role in motility in alphaproteobacteria. *J Bacteriol* **194**: 2973–2986.

Hallez, R., Bellefontaine, A.F., Letesson, J.J., and De Bolle, X. (2004) Morphological and functional asymmetry in alpha-proteobacteria. *Trends Microbiol* **12**: 361–365.

Hallez, R., Letesson, J.J., Vandenhaute, J., and Bolle, X.D. (2007a) Gateway-based destination vectors for functional analyses of bacterial ORFeomes: application to the Min system in *Brucella abortus*. *Appl Environ Microbiol* **73**: 1375–1379.

Hallez, R., Mignolet, J., Van Mullem, V., Wery, M., Vandenhaute, J., Letesson, J.J., *et al*. (2007b) The asymmetric distribution of the essential histidine kinase PdhS indicates a differentiation event in *Brucella abortus*. *EMBO J* **26**: 1444–1455.

Hartmann, E., Sommer, T., Prehn, S., Gorlich, D., Jentsch, S., and Rapoport, T.A. (1994) Evolutionary conservation of components of the protein translocation complex. *Nature* **367**: 654–657.

Holtzendorff, J., Hung, D., Brende, P., Reisenauer, A., Viollier, P.H., McAdams, H.H., and Shapiro, L. (2004) Oscillating global regulators control the genetic circuit driving a bacterial cell cycle. *Science* **304**: 983–987.

Jubier-Maurin, V., Boigegrain, R.A., Cloeckaert, A., Gross, A., Alvarez-Martinez, M.T., Terraza, A., *et al*. (2001) Major outer membrane protein Omp25 of *Brucella suis* is involved in inhibition of tumor necrosis factor alpha production during infection of human macrophages. *Infect Immun* **69**: 4823–4830.

Khan, S.R., Gaines, J., Roop, R.M., 2nd, and Farrand, S.K. (2008) Broad-host-range expression vectors with tightly regulated promoters and their use to examine the influence of TraR and TraM expression on Ti plasmid quorum sensing. *Appl Environ Microbiol* **74**: 5053–5062.

Lang, A.S., and Beatty, J.T. (2000) Genetic analysis of a bacterial genetic exchange element: the gene transfer agent of *Rhodobacter capsulatus*. *Proc Natl Acad Sci USA* **97**: 859–864.

Laub, M.T., Chen, S.L., Shapiro, L., and McAdams, H.H. (2002) Genes directly controlled by CtrA, a master regulator of the Caulobacter cell cycle. *Proc Natl Acad Sci USA* **99**: 4632–4637.

Leonard, S., Ferooz, J., Haine, V., Danese, I., Fretin, D., Tibor, A., *et al*. (2007) FtcR is a new master regulator of the flagellar system of Brucella melitensis 16M with homologs in Rhizobiaceae. *J Bacteriol* **189**: 131–141.

Magnet, S., Dubost, L., Marie, A., Arthur, M., and Gutmann, L. (2008) Identification of the l, d-transpeptidases for peptidoglycan cross-linking in *Escherichia coli*. *J Bacteriol* **190**: 4782–4785.

Manterola, L., Guzman-Verri, C., Chaves-Olarte, E., Barquero-Calvo, E., de Miguel, M.J., Moriyon, I., *et al*. (2007) BvrR/BvrS-controlled outer membrane proteins Omp3a and Omp3b are not essential for *Brucella abortus* virulence. *Infect Immun* **75**: 4867–4874.

Manterola, L., Moriyon, I., Moreno, E., Sola-Landa, A., Weiss, D.S., Koch, M.H., *et al*. (2005) The lipopolysaccharide of *Brucella abortus* BvrS/BvrR mutants contains lipid A modifications and has higher affinity for bactericidal cationic peptides. *J Bacteriol* **187**: 5631–5639.

Meinhardt, H., and de Boer, P.A. (2001) Pattern formation in *Escherichia coli*: a model for the pole-to-pole oscillations of Min proteins and the localization of the division site. *Proc Natl Acad Sci USA* **98**: 14202–14207.

Mercer, R.G., Quinlan, M., Rose, A.R., Noll, S., Beatty, J.T., and Lang, A.S. (2012) Regulatory systems controlling motility and gene transfer agent production and release in *Rhodobacter capsulatus*. *FEMS Microbiol Lett* **331**: 53–62.

Mignolet, J., Van der Henst, C., Nicolas, C., Deghelt, M., Dotreppe, D., Letesson, J.J., and De Bolle, X. (2010) PdhS, an old-pole-localized histidine kinase, recruits the fumarase FumC in *Brucella abortus*. *J Bacteriol* **192**: 3235–3239.

Moreno, E., and Moriyon, I. (2006) The genus *Brucella*. *Prokaryotes* **5**: 315–456.

Pini, F., De Nisco, N.J., Ferri, L., Penterman, J., Fioravanti, A., Brilli, M., *et al*. (2015) Cell Cycle Control by the Master Regulator CtrA in *Sinorhizobium meliloti*. *PLoS Genet* **11**: e1005232.

Pini, F., Frage, B., Ferri, L., De Nisco, N.J., Mohapatra, S.S., Taddei, L., *et al*. (2013) The DivJ, CbrA and PleC system controls DivK phosphorylation and symbiosis in *Sinorhizobium meliloti*. *Mol Microbiol* **90**: 54–71.

Pizarro-Cerda, J., Meresse, S., Parton, R.G., van der Goot, G., Sola-Landa, A., Lopez-Goni, I., *et al*. (1998a) *Brucella abortus* transits through the autophagic pathway and replicates in the endoplasmic reticulum of nonprofessional phagocytes. *Infect Immun* **66**: 5711–5724.

Pizarro-Cerda, J., Moreno, E., Sanguedolce, V., Mege, J.L., and Gorvel, J.P. (1998b) Virulent *Brucella abortus* prevents lysosome fusion and is distributed within autophagosome-like compartments. *Infect Immun* **66**: 2387–2392.

Quon, K.C., Marczynski, G.T., and Shapiro, L. (1996) Cell cycle control by an essential bacterial two-component signal transduction protein. *Cell* **84**: 83–93.

Quon, K.C., Yang, B., Domian, I.J., Shapiro, L., and Marczynski, G.T. (1998) Negative control of bacterial DNA replication by a cell cycle regulatory protein that binds at the chromosome origin. *Proc Natl Acad Sci USA* **95**: 120–125.

Reisenauer, A., Quon, K., and Shapiro, L. (1999) The CtrA response regulator mediates temporal control of gene expression during the Caulobacter cell cycle. *J Bacteriol* **181**: 2430–2439.

Robertson, G.T., Reisenauer, A., Wright, R., Jensen, R.B., Jensen, A., Shapiro, L., and Roop, R.M., 2nd (2000) The *Brucella abortus* CcrM DNA methyltransferase is essential for viability, and its overexpression attenuates intracellular replication in murine macrophages. *J Bacteriol* **182**: 3482–3489.

Salcedo, S.P., Chevrier, N., Lacerda, T.L., Ben Amara, A., Gerart, S., Gorvel, V.A., *et al*. (2013) Pathogenic *Brucella* replicate in human trophoblasts. *J Infect Dis* **207**: 1075–1083.

Shridas, P., and Waechter, C.J. (2006) Human dolichol kinase, a polytopic endoplasmic reticulum membrane protein with a cytoplasmically oriented CTP-binding site. *J Biol Chem* **281**: 31696–31704.

Sliusarenko, O., Heinritz, J., Emonet, T., and Jacobs-Wagner, C. (2011) High-throughput, subpixel precision analysis of bacterial morphogenesis and intracellular spatio-temporal dynamics. *Mol Microbiol* **80**: 612–627.

Starr, T., Child, R., Wehrly, T.D., Hansen, B., Hwang, S., Lopez-Otin, C., *et al*. (2012) Selective subversion of

autophagy complexes facilitates completion of the *Brucella* intracellular cycle. *Cell Host Microbe* **11**: 33–45.
Starr, T., Ng, T.W., Wehrly, T.D., Knodler, L.A., and Celli, J. (2008) *Brucella* intracellular replication requires trafficking through the late endosomal/lysosomal compartment. *Traffic* **9**: 678–694.
Stouf, M., Meile, J.C., and Cornet, F. (2013) FtsK actively segregates sister chromosomes in *Escherichia coli*. *Proc Natl Acad Sci USA* **110**: 11157–11162.
Terwagne, M., Mirabella, A., Lemaire, J., Deschamps, C., De Bolle, X., and Letesson, J.J. (2013) Quorum sensing and self-quorum quenching in the intracellular pathogen *Brucella melitensis*. *PLoS One* **8**: e82514.
Van der Henst, C., de Barsy, M., Zorreguieta, A., Letesson, J.J., and De Bolle, X. (2013) The *Brucella* pathogens are polarized bacteria. *Microbes Infect* **15**: 998–1004.
Vanderlinde, E.M., and Yost, C.K. (2012) Mutation of the sensor kinase chvG in *Rhizobium leguminosarum* negatively impacts cellular metabolism, outer membrane stability, and symbiosis. *J Bacteriol* **194**: 768–777.
Wheeler, R.T., and Shapiro, L. (1999) Differential localization of two histidine kinases controlling bacterial cell differentiation. *Mol Cell* **4**: 683–694.
Willett, J.W., Herrou, J., Briegel, A., Rotskoff, G., and Crosson, S. (2015) Structural asymmetry in a conserved signaling system that regulates division, replication, and virulence of an intracellular pathogen. *Proc Natl Acad Sci USA* **112**: E3709–E3718.
Zweiger, G., Marczynski, G., and Shapiro, L. (1994) A *Caulobacter* DNA methyltransferase that functions only in the predivisional cell. *J Mol Biol* **235**: 472–485.

Supporting information

Additional supporting information may be found in the online version of this article at the publisher's web-site.